

# VAE Approximation Error: ELBO and Conditional Independence

Dmitrij Schlesinger<sup>\*1</sup> Alexander Shekhovtsov<sup>\*2</sup> Boris Flach<sup>\*2</sup>

## Abstract

The importance of Variational Autoencoders reaches far beyond standalone generative models — the approach is also used for learning latent representations and can be generalized to semi-supervised learning. This requires a thorough analysis of their commonly known shortcomings: posterior collapse and approximation errors. This paper analyzes VAE approximation errors caused by the combination of the ELBO objective with the choice of the encoder probability family, in particular under conditional independence assumptions. We identify the subclass of generative models consistent with the encoder family. We show that the ELBO optimizer is pulled from the likelihood optimizer towards this consistent subset. Furthermore, this subset can not be enlarged, and the respective error cannot be decreased, by only considering deeper encoder networks.

## 1. Introduction

Variational autoencoders proposed by Kingma & Welling (2014) strive at learning complex data distributions  $p(x)$ ,  $x \in \mathcal{X}$  from given i.i.d. data in a generative way. To achieve this goal, they introduce latent variables  $z \in \mathcal{Z}$  and model the joint distribution as  $p_\theta(x|z)p(z)$ , where  $p(z)$  is a simple distribution that is usually assumed to be known. The complex conditional distribution (aka *decoder*)  $p_\theta(x|z)$  parametrized by  $\theta \in \Theta$  is often modeled in terms of a deep network. Models defined in this way allow to sample from  $p_\theta(x) = \mathbb{E}_{p(z)}p_\theta(x|z)$  easily, however at the price that computing the posterior  $p_\theta(z|x) = p_\theta(x|z)p(z)/p_\theta(x)$  is usually intractable. To handle this problem, especially when learning the model, VAEs approximate the posteriors  $p_\theta(z|x)$  by an amortized inference model (aka *encoder*)  $q_\phi(z|x)$  parametrized by  $\phi \in \Phi$ . Given the empirical data distribution  $p_d(x)$ , the model is learned by maximizing the

<sup>\*</sup>Equal contribution <sup>1</sup>Dresden University of Technology  
<sup>2</sup>Czech Technical University in Prague. Correspondence to: Dmitrij Schlesinger <Dmytro.Schlesinger@tu-dresden.de>.

evidence lower bound (ELBO) of the data log-likelihood  $L(\theta) = \mathbb{E}_{p_d} \log p_\theta(x)$ . The ELBO can be expressed in the following two equivalent forms:  $L_B(\theta, \phi) =$

$$\mathbb{E}_{p_d} [\mathbb{E}_{q_\phi} \log p_\theta(x|z) - D_{\text{KL}}(q_\phi(z|x) \| p(z))] \quad (1a)$$

$$= L(\theta) - \mathbb{E}_{p_d} [D_{\text{KL}}(q_\phi(z|x) \| p_\theta(z|x))]. \quad (1b)$$

The first form allows for stochastic optimization of ELBO while the second form allows to see that the gap between log-likelihood and ELBO is exactly the mismatch between the encoder and the posterior.

The importance of VAEs reaches far beyond standalone models for data generation. With some modifications they can be used as generative models for classification, enabling *e.g.* their semi-supervised learning. Moreover, a similar approach is used in variational Bayesian inference, *e.g.* when the network parameters are assumed to be random variables. The outreach of the VAE approach requires therefore a careful empirical and theoretical analysis of the problems it may suffer from. The most important ones are (i) posterior collapse and (ii) approximation errors caused by an inappropriate choice of the encoder family  $\mathcal{Q}_\Phi$ .

Posterior collapse in VAE optimization manifests in collapse of the encoder  $q_\phi(z_i|x)$  towards the prior  $p(z_i)$  for some components  $z_i$  of the latent variable  $z$ . The same holds for the corresponding decoder posteriors  $p_\theta(z_i|x)$ . These collapsed latent components hold no information about  $x$ . Posterior collapse has been studied extensively both empirically and theoretically. Partial posterior collapse was found to correspond to local optima of ELBO and can be partially avoided by training the encoder more aggressively (He et al., 2019). Notably, Lucas et al. (2019); Dai et al. (2018) show that the ELBO criterion for *linear* Gaussian VAEs introduces no additional local optima to the data log-likelihood. Moreover at the global optimum of ELBO for deep Gaussian VAEs the number of non-collapsed dimensions estimates the dimensionality of the data manifold (Dai & Wipf, 2019). These works consider VAEs with continuous latent spaces. In discrete VAEs, to our knowledge, the posterior collapse is relatively less understood.

The second important issue of VAEs is the approximation error caused by an inappropriate choice of the encoder family and the resulting mismatch between the en-

coder and the model posterior. It has been studied (e.g., Cremer et al. 2018; Hjelm et al. 2016; Kim et al. 2018) so far mainly empirically. The problem also occurs and is well-recognized in the context of variational inference and variational Bayesian inference, where the target posterior distribution is expected to be complex. Several works proposed enriched encoder families for VAEs, keeping the ELBO objective tractable at the same time. For instance, Burda et al. (2016) introduce a family of tighter bounds using importance weighting, Kingma et al. (2016) combine Gaussian models with inverse autoregressive flows and Sønderby et al. (2016) consider hierarchical or ladder VAEs. However, Rainforth et al. (2018) show that tighter lower bounds such as IWAE (Burda et al., 2016) lead to lower signal-to-noise ratio in gradient estimators, making learning more difficult. In addition, in VAEs, unlike in variational inference, the decoder may adopt to compensate for the chosen encoder family and the effect of this coupling, we believe, is not fully understood.

The aim of this paper is to study the approximation error of VAEs theoretically and to identify its underlying conceptual reasons. We consider VAEs with encoders from an exponential family, in particular factorizing encoders, and identify the subclass of generative models that are consistent with such encoders. We show that the ELBO optimizer for such VAEs is pulled from the likelihood optimizer towards this consistent subset and analyze the question whether it can be enlarged by choosing more complex encoder networks.

## 2. Problem Statement

We adopt the following notion of approximation error. Given a generative model class  $\mathcal{P}_\Theta = \{p_\theta(x, z) \mid \theta \in \Theta\}$  and an encoder class  $\mathcal{Q}_\Phi = \{q_\phi(z \mid x) \mid \phi \in \Phi\}$ , we define the *consistent set*  $\mathcal{P}_\Theta(\mathcal{Q}_\Phi) \subseteq \mathcal{P}_\Theta$  as the subset of distributions  $p_\theta(x, z)$  whose posteriors are in  $\mathcal{Q}_\Phi$ , i.e.  $\mathcal{P}_\Theta(\mathcal{Q}_\Phi) =$

$$\{p_\theta(x, z) \in \mathcal{P}_\Theta \mid \exists \phi \in \Phi : q_\phi(z \mid x) \equiv p_\theta(z \mid x)\}. \quad (2)$$

Let us consider the case that  $\mathcal{P}_\Theta(\mathcal{Q}_\Phi)$  is a strict subset of  $\mathcal{P}_\Theta$ . The KL-divergence in the ELBO objective (1b) can vanish only if  $p_\theta \in \mathcal{P}_\Theta(\mathcal{Q}_\Phi)$ . If the likelihood maximizer

$$\theta^* \in \operatorname{argmax}_{\theta \in \Theta} \mathbb{E}_{p_d(x)} \log p_\theta(x) \quad (3)$$

is not contained in  $\mathcal{P}_\Theta(\mathcal{Q}_\Phi)$ , then this KL-divergence will obviously pull the optimizer towards  $\mathcal{P}_\Theta(\mathcal{Q}_\Phi)$ , even for an optimal encoder. Fig. 1 illustrates this schematically. For an autoencoder with parameters  $(\theta, \phi)$  we define the *approximation error* as

$$\mathbb{E}_{p_d(x)} [\log p_{\theta^*}(x) - \log p_\theta(x)]. \quad (4)$$

In order for this error to become zero two conditions need to be satisfied:

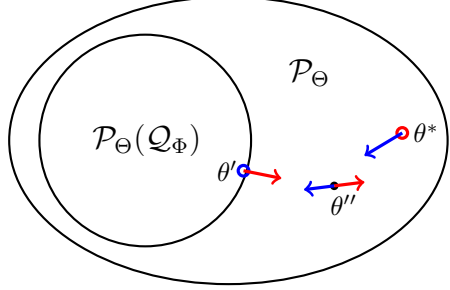


Figure 1. In a general case,  $\mathcal{P}_\Theta(\mathcal{Q}_\Phi)$  is a strict subset of  $\mathcal{P}_\Theta$  and the decoder model  $p_{\theta^*}(x, z)$  optimizing data log-likelihood is outside this subset. Gradients of the data log-likelihood (red) and of the function  $F(\theta) = \min_{\phi} \mathbb{E}_{p_d} D_{\text{KL}}(q_\phi(z \mid x) \parallel p_\theta(z \mid x))$  (blue) are shown for the points  $\theta^*$ ,  $\theta'$  and  $\theta''$ , where  $\theta'$  is the model with the best data log-likelihood in  $\mathcal{P}_\Theta(\mathcal{Q}_\Phi)$  and  $\theta''$  is the ELBO optimizer. Zero gradients are depicted by small circles.

- Parameters  $(\theta, \phi)$  must be optimal for the ELBO objective.
- ELBO should be *tight* at  $(\theta, \phi)$ , i.e.,  $L_B(\theta, \phi) = L(\theta)$ .

Because the non-tightness gap  $L(\theta) - L_B(\theta, \phi)$  expresses as  $\mathbb{E}_{p_d} [D_{\text{KL}}(q_\phi(z \mid x) \parallel p_\theta(z \mid x))]$  from (1b) and KL-divergence is non-negative for every  $x$ , a necessary precondition for tightness is that the *amortization gap* is zero, i.e. for all  $x$  there is no better inference model  $q$  for this  $x$  alone (as in non-amortized stochastic variational inference). This gap can be the dominating source of error, as experimentally shown by Cremer et al. (2018). A common remedy is to consider a sufficiently complex neural network for the encoder. However, the probabilistic family of the encoder also needs to be sufficiently expressive in order to achieve tightness. We consider a general class of VAEs, where both encoder and decoder are defined as exponential families. This class includes many common models, in particular Gaussian VAEs and Bernoulli VAEs with the usual conditional independence assumptions. We characterize their consistent set  $\mathcal{P}_\Theta(\mathcal{Q}_\Phi)$ , on which the bound achieves tightness, and show that this set is quite narrow and does not depend on the complexity of the encoder and decoder networks beyond simple 1-layer linear mappings of sufficient statistics.

## 3. Characterization of Tight VAEs

We theoretically investigate under what conditions the approximation error of VAE can be made exactly zero. As discussed above, a tight VAE must satisfy

$$\forall (x, z) \quad q_\phi(z \mid x) = p_\theta(z \mid x). \quad (5)$$

We assume also that both encoder and decoder are exponential families employing arbitrarily complex networks. The following theorem is our main theoretical result that allows to characterize tight VAEs in this setting.

**Theorem 1.** Let  $x \in \mathcal{X}$  and  $z \in \mathcal{Z}$  be random variables with a strictly positive joint distribution such that both conditional distributions are exponential families with densities in the minimal representation

$$p(x | z) = h(x) \exp[\langle \nu(x), f(z) \rangle - A(z)] \quad (6a)$$

$$p(z | x) = h'(z) \exp[\langle \psi(z), g(x) \rangle - B(x)], \quad (6b)$$

where  $\nu : \mathcal{X} \rightarrow \mathbb{R}^n$  and  $\psi : \mathcal{Z} \rightarrow \mathbb{R}^m$  are minimal sufficient statistics,  $f : \mathcal{Z} \rightarrow \mathbb{R}^n$  and  $g : \mathcal{X} \rightarrow \mathbb{R}^m$  are any mappings,  $h(x)$  and  $h'(z)$  are base measures, and  $A(z)$  and  $B(x)$  denote the respective log-partition functions.

Then there exists a matrix  $W \in \mathbb{M}(n+1, m+1)$ , such that the density of the joint distribution can be represented as

$$p(x, z) = h(x)h'(z) \exp \langle \nu_e(x), W\psi_e(z) \rangle, \quad (7)$$

where  $\nu_e, \psi_e$  denote the statistics vectors extended with an additional component 1.

*Proof.* The minimal representation assumption ensures that the affine hulls of  $\{\nu(x) \mid x \in \mathcal{X}\}$  and  $\{\psi(z) \mid z \in \mathcal{Z}\}$  coincide with the entire respective Euclidean spaces. By taking the logarithm of the equation

$$\frac{p(x | z)p(z)}{h(x)h'(z)} = \frac{p(z | x)p(x)}{h(x)h'(z)} \quad \forall x \in \mathcal{X}, \forall z \in \mathcal{Z}. \quad (8)$$

and substituting (6), we obtain the system of equations

$$\langle \nu(x), f(z) \rangle + a(z) = \langle \psi(z), g(x) \rangle + b(x) \quad (9)$$

for all  $x \in \mathcal{X}, z \in \mathcal{Z}$ , where

$$a(z) = \log p(z) - A(z) - \log h'(z), \quad (10a)$$

$$b(x) = \log p(x) - B(x) - \log h(x). \quad (10b)$$

We represent the system (9) more compactly by extending the Euclidean spaces by one dimension and extending the respective mappings as

$$\nu(x) \rightarrow (\nu(x), 1), \quad f(z) \rightarrow (f(z), a(z)), \quad (11a)$$

$$\psi(z) \rightarrow (\psi(z), 1), \quad g(x) \rightarrow (g(x), b(x)). \quad (11b)$$

Using this extension and redefining  $n \rightarrow n+1$  and  $m \rightarrow m+1$ , we have

$$\langle \nu(x), f(z) \rangle = \langle \psi(z), g(x) \rangle \quad \forall x \in \mathcal{X}, \forall z \in \mathcal{Z}. \quad (12)$$

The sets  $\nu(\mathcal{X})$  and  $\psi(\mathcal{Z})$  span the respective (extended by 1) Euclidean spaces, i.e.  $\text{span}\{\nu(x) \mid x \in \mathcal{X}\} = \mathbb{R}^n$  and  $\text{span}\{\psi(z) \mid z \in \mathcal{Z}\} = \mathbb{R}^m$ . This follows from the properties of the affine hulls in the original Euclidean spaces. Therefore we can choose  $n$  points  $x_i \in \mathcal{X}$  such that vectors  $\nu_i = \nu(x_i)$  define a basis in  $\mathbb{R}^n$  and similarly  $m$  points  $z_j \in \mathcal{Z}$  such that vectors  $\psi_j = \psi(z_j)$  define a basis in  $\mathbb{R}^m$ .

Let  $\nu_i^*$  and  $\psi_j^*$  denote the respective dual bases. Representing  $f(z) \in \mathbb{R}^n$  and  $g(x) \in \mathbb{R}^m$  in the respective bases and using (12), we obtain

$$f(z) = \sum_i \langle \nu_i, f(z) \rangle \nu_i^* = \sum_i \langle \psi(z), g(x_i) \rangle \nu_i^*, \quad (13)$$

$$g(x) = \sum_j \langle \psi_j, g(x) \rangle \psi_j^* = \sum_j \langle \nu(x), f(z_j) \rangle \psi_j^*. \quad (14)$$

Taking the l.h.s. of (12), substituting  $f(z)$  by r.h.s. of (13) and then  $g(x_i)$  by (14), we get

$$\langle \nu(x), f(z) \rangle = \langle \nu(x), W\psi(z) \rangle, \quad (15)$$

where the  $n \times m$  matrix  $W$  is given by

$$W = \sum_{i,j} \langle \nu_i, f(z_j) \rangle \nu_i^* \otimes \psi_j^*. \quad (16)$$

This proves for all  $x, z$  that the logarithm of expression (8) equals  $\langle \nu_e(x), W\psi_e(z) \rangle$ , where  $\nu_e$  and  $\psi_e$  are the extended sufficient statistics obtained from the original ones by (11). The form of the joint density (7) follows.  $\square$

*Remark 1.* Notice that the theorem imposes no restrictions on the nature of random variables  $x$  and  $z$ . They can be discrete or continuous, univariate or multivariate.

*Remark 2.* The strict positiveness assumption can be dropped if both  $x$  and  $z$  are discrete random variables. Indeed,  $p(x | z)$  can be zero only if the base measure is zero, i.e., independently of  $z$ . We can therefore consider the respective subsets of  $\mathcal{X}, \mathcal{Z}$ , where the base measures are strictly positive. The theorem applies to the positive distributions on these subsets.

For a tight optimal VAE, **Theorem 1** implies that the joint distribution takes form (7), which can be parametrized by a single matrix  $W$  instead of the complex neural networks with parameters  $\theta, \phi$ . The respective conditional distributions then belong to the class of *generalized linear models* (GLMs). Indeed, e.g., the encoder  $q_\phi(z | x)$  must be in the exponential family

$$p(z | x) = h'(z) \exp(\langle \psi_e(z), g(x) \rangle - B(g(x))) \quad (17)$$

with natural parameters  $g(x) = W^\top \nu_e(x)$ , and similarly for the decoder. Thus the mappings  $f$  and  $g$  must degenerate to this linear regime in the space of sufficient statistics.

The theorem also implies a guarantee of tightness if we constrain the decoder from the very beginning.

**Corollary 1.** Let the decoder network family be affine in  $\psi(z)$ , i.e.,  $f(z) = W\psi(z) + a$  and let the encoder network family  $g(x)$  include at least all affine maps  $V\nu(x) + b$ . Then any global optimum of ELBO attains a zero approximation error.

*Proof.* For a given optimal VAE  $(\theta, \phi)$ , the true posterior is guaranteed to be in the encoder class and thus  $\exists \phi'$  such that VAE  $(\theta, \phi')$  is tight. Since  $\phi$  is optimal, it must also attain zero posterior KL divergence. Therefore we have  $L_B(\theta, \phi) = L(\theta)$  and the claim follows.  $\square$

In practice, VAE models are almost never tight. Nevertheless, as discussed in Section 2 the ELBO objective pulls the optimizer away from the maximum likelihood solution towards the subset  $\mathcal{P}_\Theta(\mathcal{Q}_\Phi)$ . This subset of consistent models can not be enlarged by considering more complex encoder networks  $g(x)$  as long as the affine family  $W\nu_e(x)$  can already be represented. We also observe that the influence on the learned decoder is that it is pulled towards the simple joint distribution (7), constituting an inductive bias which may be interpreted as a useful regularization or as a harmful effect, depending on the application and on whether the simple joint distribution (7) makes a meaningful baseline.

A common choice to define a tractable VAE model is to use a conditionally independent encoder and decoder. Let  $q(z|x) = \prod_j q(z_j|x)$ . Let also  $q(z_j|x) = h'(z_j) \exp(\psi_j(z_j)^\top g_\phi(x)_j - B_j(g_\phi(x)_j))$  be an exponential family with minimal sufficient statistics  $\psi_j(z_j)$ . Since optimizing ELBO in  $q$  is equivalent to minimizing  $D_{\text{KL}}(q_\phi(z|x) \parallel p_\theta(z|x))$ , the optimal solution is at best<sup>1</sup> the *mean field approximation* to  $p_\theta(z|x)$ , as in stochastic variational inference (Hoffman et al., 2013). It is known that optimizing the decoder in turn, pulls it towards having a factorized posterior. Theorem 1 gives a more detailed view, that the decoder is pulled towards having  $f(x) = W\psi(z) + u$ , where  $\psi(z)$  is the concatenation of all sufficient statistics  $\psi_j(z_j)$ . In a simple case when  $\psi_j(z_j) = z_j$ , towards a simple linear model  $f(x) = Wz + u$ .

### 3.1. Case Studies

In this subsection we apply Theorem 1 to three representative types of VAEs and analyze its consequences.

**Example 1** (Diagonal Gaussian VAE). Let us consider a Gaussian VAE, as commonly applied to image generation. Let  $\mathcal{X} = \mathbb{R}^n$ ,  $\mathcal{Z} = \mathbb{R}^m$ ,  $p(x|z) = \mathcal{N}(x|\mu_d(z), \sigma_d^2 I)$ ,  $q(z|x) = \mathcal{N}(z|\mu_e(x), \text{diag}(\sigma_e^2(x)))$ , where  $\mu_d$ ,  $\mu_e$  and  $\sigma_e$  are suitable (convolutional) neural networks and  $\sigma_d$  is a common pixel observation noise parameter. The decoder has minimal sufficient statistics  $\nu(x) = x$  and the base measure  $h(x) = \mathcal{N}(x|0, \sigma^2 I)$ . The encoder has minimal sufficient statistics  $\psi(z) = (z, z^2)$ , where the square is coordinate-wise. Theorem 1 implies that a tight optimal VAE matches the joint model  $p(x, z) \propto$

$$h(x) \exp(\langle x, Wz + Vz^2 + a \rangle + \langle b, z \rangle + \langle c, z^2 \rangle) \quad (18)$$

for some matrices  $W, V$  and vectors  $a, b, c$  of suitable size. Furthermore, the integral over  $z$  must be finite for all  $x$  and therefore  $x^\top V + c < 0$  must hold for all  $x \in \mathbb{R}^n$ . This is possible only if  $V = 0$  and  $c < 0$ . The joint distribution is therefore a multivariate Gaussian and the same

<sup>1</sup>When the amortization gap is eliminated by using a sufficiently large encoder network  $g$ .

holds for its marginal  $p(x)$ . The neural network  $\mu_d(z)$  must degenerate to  $\mu_d(z) = \sigma_d^2 \cdot (Wz + a)$  and the two neural networks for the encoder to  $\sigma_e^2(x) = -1/2c$  and  $\mu_e(x) = -(W^\top x + b)/2c$ , where divisions are coordinate-wise. VAEs with such simplified, linear Gaussian encoder-decoder pairs are known to be tight and to match the probabilistic PCA model (Dai et al., 2018; Lucas et al., 2019).

In Section 4 we study this case experimentally and show that optimizing ELBO for a general decoder network  $\mu_d$  pushes the decoder towards such a simple model and causes qualitative and quantitative degradation.

**Example 2** (Bernoulli VAE). Another case often studied in the literature is discrete VAE models and more specifically binary ones (Grathwohl et al., 2018; Tucker et al., 2017; Yin & Zhou, 2019).

Let  $x \in \{-1, 1\}^n$  and  $z \in \{-1, 1\}^m$  be binary valued random vectors. It is commonly assumed that  $p(x|z)$  and  $q(z|x)$  are conditionally independent models. In this case their respective sufficient statistics are just the vectors  $\nu(x) = x$  and  $\psi(z) = z$ . Note how the exponential family framework seamlessly accounts for the assumed conditional factorization of the encoder and decoder through vector-valued sufficient statistics. By Theorem 1, the joint distribution of a tight optimal VAE must take the form

$$p(x, z) = \frac{1}{c} \exp(x^\top Wz + u^\top x + v^\top z), \quad (19)$$

which is the restricted Boltzmann machine (RBM), a well-known and well-studied model with many applications.

Consequently, the (marginal) data distribution  $p(x)$  has the form

$$p(x) = \frac{2^m}{c} \exp[\langle u, x \rangle] \prod_{j=1}^m \cosh(\langle w_j^\top, x \rangle + v_j), \quad (20)$$

where  $w_j^\top$  denotes the  $j$ -th row vector of the transposed matrix  $W^\top$ . The first term factors in components of  $x$ . Any correlation between components of  $x$  is therefore caused by the second term. Each factor  $\cosh(\langle w_j^\top, x \rangle + v_j)$  of it represents an essentially one-dimensional function with constant gradient direction  $w_j^\top$ .

**Example 3** (Bernoulli VAE for Semantic Hashing). One important application of Bernoulli VAEs is the *semantic hashing* problem, initially proposed and modeled with RBMs (Salakhutdinov & Hinton, 2009). The problem is to assign to each document / image a compact binary latent code that can be used for a quick retrieval by nearest neighbor search. We will detail now a more recent VAE model for text documents (Chaidaroon & Fang, 2017; Shen et al., 2018) and show that it can be tight only in a full posterior collapse. We correct the encoder so as to allow a larger consistent set and observe that the resulting consistent joint distribution matches RBM.

Let  $x \in \mathbb{N}^K$  be word counts in a document with words from a dictionary of size  $K$ . Let  $z \in \{0, 1\}^m$  be a binary latent code of a document. Let  $l = \sum_k x_k$  denote the document's length. We assume that the document length is independent of the latent topic and its distribution  $p(l)$  can be learned separately (*e.g.*, a log-normal distribution is a good fit). The decoder is defined using the multinomial distribution model (words in the document are drawn from the same categorical distribution corresponding to its topic):

$$p(x, l | z) = p(l)h(x | l) \exp(f(z)^\top x - lA(f(z))), \quad (21)$$

where  $f(z)$  is a neural network mapping latent code to the logits of word occurrence probabilities,  $A(\eta) = \log \sum_k \exp(\eta_k)$  and  $h(x | l) = [\sum_k x_k = l] (l! / \prod_k x_k!)$  is the base measure<sup>2</sup>. The sufficient statistics are the word counts  $x$ . The prior  $p(z)$  is assumed uniform Bernoulli.

The encoder is the conditionally independent Bernoulli model, expressed as

$$q(z | x, l) \propto \exp(g(x)^\top z), \quad (22)$$

where  $g(x)$  is the encoder network. Chaidaroon & Fang (2017) experimented with the encoder and decoder design and recommended using TFIDF features instead of raw counts. First, we note that the inverse document frequency (IDF) is not relevant, since it can be learned by the first linear transform in the encoder. Effectively, the term frequency (TF), given by  $x/l$ , is used. This choice is adopted in later works (Shen et al., 2018; Zamani Dadaneh et al., 2020; Nanculef et al., 2020). It might seem reasonable that the latent code modeling the document topic should not depend on the document length, only on the distribution of words in the document. However, we will argue that this rationale is misleading for stochastic encoders.

We apply Theorem 1 to two groups of variables: observed  $(x, l)$  and latent  $z$  with  $h(x, l) = h(x | l)p(l)$ ,  $\nu(x, l) = x$  and  $\psi(z) = z$ . It follows that the joint distribution of a tight VAE must take the form:

$$p(x, l, z) = h(x, l) \exp(x^\top Wz + a^\top x + b^\top z + c). \quad (23)$$

This however implies that  $g(x) = Wx + b$ , *i.e.* the encoder network must be linear in  $x$ . Consequently, it cannot match a function of word frequencies  $x/l$  (as chosen by design) unless  $W = 0$ , *i.e.* a completely trivial model with an encoder not depending on  $x$ . Such an encoder would imply full posterior collapse. We conjecture that the inherent inconsistency of this VAE has a detrimental effect on learning.

If instead, we let the encoder network to access word counts  $x$  directly, we obtain that  $g(x) = Wx + b$  can form a tight

<sup>2</sup>Prior work (Chaidaroon & Fang, 2017; Shen et al., 2018) omit the base measure as it has no trainable parameters.

VAE. Inspecting this encoder model in more detail, we see that it builds up confidence in proportion to the evidence (total word counts), as the true posterior would. Indeed, the true posterior  $p(z | x, l)$  satisfies the factorization by Bayes's theorem:  $p(z | x, l) = p(x | z, l)p(z) / p(x | l)$ . The prior  $p(z)$  is constant by design,  $p(x | l)$  does not vary with  $z$  and  $p(x | z, l)$  factors over all word instances according to (21). In other words, the coupling between  $x$  and  $z$  in  $\log p(z | x, l)$  is linear in  $x$ .

In Section 4 we study the proposed correction experimentally and show that it enables learning better models under a variety of settings.

### 3.2. Relation to Prior Work

The simplified model of the decoder and encoder that we obtained in Example 1 coincides with the "linear VAE" class of models studied by Lucas et al. (2019). They show that in this case the likelihood matches that of the pPCA model and that the ELBO is tight (Lucas et al., 2019, Lemma 1). Our Corollary 1 is a generalization of their Lemma 1 to decoders in any exponential family with natural parameters being a linear mapping of any fixed lifted latent representation  $\psi(z)$ .

Cremer et al. (2018) showed experimentally that using a more expressive class of models for the encoder reduces not only the posterior family mismatch but also the amortization error. This observation is compatible with our theorem: increasing the expressive power of the encoder alone admits tight VAEs with more complex dependence of  $z$  on  $x$ . Indeed, increasing the expressive power of the encoder in our setting means extending its sufficient statistics  $\psi(z)$  by new components. While this does not enrich the linear dependence  $g(x) = W^\top \nu(x)$  characterizing tight VAEs, it does lead to a more expressive GLM  $p(z | x)$ . In particular it has a more expressive link function describing the dependence of  $\mathbb{E}[z | x]$  on  $x$ . Conversely, our results suggest that increasing the complexity of the encoder network in order to reduce the amortization gap is only useful for models that are far from the consistent set.

Dai & Wipf (2019, Theorem 2) show, for a class of Gaussian VAEs with general neural networks  $f_\theta, g_\phi$ , that it is possible to build a sequence of network parameters  $\theta_t, \phi_t$  in order to approximate the target distribution arbitrary well, including that the posterior mismatch  $D_{\text{KL}}(q_{\phi_t}(z | x) \| p_{\theta_t}(z | x))$  approaches zero, *i.e.*, the VAE asymptotically approaches tightness. To achieve this, the neural networks  $f_\theta, g_\phi$  must be general enough to implement a smooth invertible mapping, transforming the standard multivariate Gaussian prior distribution into the target distribution. However, since both encoder and decoder stay Gaussian, our Theorem 1 implies that for a tight VAE of this type, the mappings  $f_\theta, g_\phi$  must be simple, in par-

ticular  $g_\phi$  must be linear in  $x$ . A contradiction does not occur because in the above mentioned limit both the decoder and encoder approach deterministic mappings which are not exponential families. We believe that the deterministic encoder-decoder setting is a special case<sup>3</sup> and if, *e.g.*, the variance of  $p_\theta(z|x)$  is bounded away from zero, a model that approaches tightness should also approach the form described by [Theorem 1](#). Showing this exactly under appropriate assumptions is left for future work.

[Sicks et al. \(2021\)](#) derive several results allowing to analyze ELBO (and in particular the posterior collapse problem) which hold locally under the assumption that the decoder’s mapping  $f(z)$  is an affine mapping of  $z$ . Our [Theorem 1](#) implies it must be so (globally) for tight VAEs in several special cases (*e.g.*, Bernoulli model), while in general it is an affine mapping of  $\psi(z)$ . These connections indicate that a better understanding of VAEs can be reached in the setting where either decoder or encoder or both are consistent with the joint model (7).

## 4. Experiments

### 4.1. Artificial Example

To start with, we illustrate our findings on a toy example. We consider a simple Gaussian mixture model for which we can easily generate samples and compute all necessary quantities. We define the ground truth model to be  $p^*(x, z) = p^*(z)p^*(x|z)$ , with  $z \in \{1 \dots 4\}$ ,  $p^*(z) = 0.25$ ,  $x \in \mathbb{R}^2$ ,  $p^*(x|z) = \mathcal{N}(x|\mu(z), \sigma^2 I)$ , *i.e.* a mixture of four 2D Gaussians. [Fig. 2\(a\)](#) shows the color-coded posterior distribution  $p^*(z|x)$ . We assign a color to each component from 1 to 4 and represent  $p^*(z|x)$  for each pixel  $x \in \mathbb{R}^2$  by the corresponding mixture of the component colors. For better interpretability, we illustrate further results by decision maps  $\arg \max_z p(z|x)$ . [Fig. 2\(b\)](#) shows the decision map for  $p^*(z|x)$ . The negative entropy  $\sum_x p^*(x) \log p^*(x)$  of the ground truth model, *i.e.* the best reachable data log-likelihood, is  $-3.65$ .

The aim of the experiment is to learn a VAE and to study the influence of the factorization assumption on the results. We use the decoder architecture as in the ground truth model — a Gaussian distribution  $p_\theta(x|z) = \mathcal{N}(x|\theta z_{oh}, \sigma^2 I)$ , where  $z_{oh}$  is the one-hot (categorical) representation of  $z$ , and  $\theta$  is a  $2 \times 4$  matrix that allows to map the four latent codes to 2D centers at general locations. We restrict the encoder to factor over the binary representation of the code  $z_b \in \{0, 1\}^2$  and define it as  $q_\phi(z_b|x) \propto \exp \langle g_\phi(x), z_b \rangle$ , where  $g_\phi(x)$  is implemented as a feed-forward network with two hidden layers, each with 64 units and ReLU activations.

<sup>3</sup>Corresponding to the invertible neural network approach.

First, we pre-train our factorized encoder by optimizing ELBO and keeping the ground truth decoder fixed. The goal of this step is to investigate the approximation quality of the true posterior by a factorized one. The decision map for the pre-trained encoder is shown in [Fig. 2\(c\)](#). The impact of the factorization is clearly visible — one can see two decision boundaries (one for each bit of  $z_b$ ), which together partition the  $x$ -space into four regions, approximating the true posterior. Notice also the explanation given in [Fig. 2\(f\)](#). The ELBO of the pre-trained VAE is  $-3.74$ .

The next step is to jointly train the encoder and decoder by maximizing ELBO. We start with the ground truth decoder and the pre-trained encoder from the previous step. The ELBO-optimal decoder has to match not only the training data, but also the inexact, factorizing encoder. The resulting  $q_\phi(z|x)$  is shown in [Fig. 2\(d\)](#) and the learned decoder posterior  $p_\theta(z|x) \propto p(z)p_\theta(x|z)$  in [Fig. 2\(e\)](#). Note that they match each other pretty well, but differ substantially from the ground truth posterior shown in [Fig. 2\(b\)](#). Quantitatively, the ELBO value increases during this training from  $-3.74$  to  $-3.70$ . The data log-likelihood  $\sum_x p^*(x) \log p_\theta(x)$  drops at the same time from  $-3.65$  to  $-3.68$ . Thus the approximation error (4) in the decoder caused by using the factorized encoder is only 0.03 nats, but the qualitative difference in [Fig. 2](#) appears detrimental.

Summarizing, this simple toy example clearly shows the VAE approximation error caused by the combination of ELBO objective and the factorization assumption for the encoder.

### 4.2. Gaussian VAEs for CelebA Images

The layout of this experiment is similar to the previous one. We first define a ground truth decoder which is used to generate training images. Then we pre-train an encoder by ELBO keeping the ground truth decoder fixed. Finally, we train both model parts starting from the ground truth decoder and the pre-trained encoder.

The ground truth generative model is obtained as follows. First, we train a convolutional Generative Adversarial network (GAN) using code of [Inkawich \(2017\)](#) on the CelebA dataset. We scale and crop all images to  $64 \times 64$  pixels. In order to get a stochastic decoder, we equip the GAN generator  $x = d(z)$ ,  $z \in \mathbb{R}^{100}$ ,  $x \in \mathbb{R}^{64 \times 64 \times 3}$  with *image noise*  $\sigma_d$ . To summarize, the ground truth generative model is defined as  $p^*(x, z) = p^*(z)p^*(x|z)$ , where  $p^*(z) = \mathcal{N}(z|0, I)$ ,  $p^*(x|z) = \mathcal{N}(x|\mu_d(z), \sigma_d^2 I)$ , and  $\sigma_d^2$  is a common noise variance for all pixels and color channels and does not depend on  $z$ . In our experiments we chose  $\sigma_d = 0.05$  (the color values are normalized to  $[-1, 1]$ ). This corresponds to an image noise level, which is just visible, but does not disturb visual perception essentially.

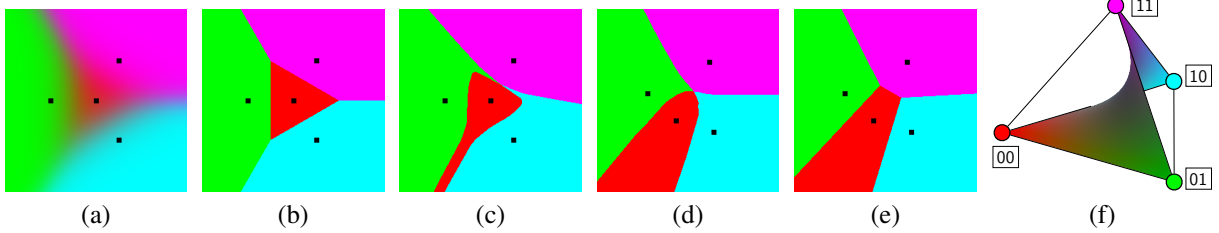


Figure 2. Artificial example (see text for details). (a) Color-coded posterior distribution  $p^*(z|x)$ . (b-e): Decision maps ( $\arg \max_z$ ) of: (b) true posterior  $p^*(z|x)$ , (c) encoder posterior  $q_\phi(z|x)$  after pre-training encoder with the fixed ground truth decoder, (d) encoder posterior  $q_\phi(z|x)$  after joint learning, (e) decoder posterior  $p_\theta(z|x)$  after joint learning. Gaussian centers  $\mu(z)$  are shown as black dots. (f) Probability simplex of distributions over the four binary configurations. The vertices correspond to pure (deterministic) binary states represented by the code and its respective color. The surface shows the manifold of factorized distributions realizable by  $q(z|x)$ . Notice that the two edges  $(00, 11)$  and  $(01, 10)$  are not in the manifold because they correspond to switching of two bits simultaneously in a correlated way. The factorized approximation cannot model transitions between these states. Hence, when learning VAE, these pairs of states are repulsed in the encoder decision maps (c), (d).



Figure 3. Results for the encoder learned by supervised conditional likelihood. Top row: training samples  $\hat{x} \sim p^*(x)$ . Second row: the corresponding reconstructions from mean values of  $z$ , i.e.  $x \sim p^*(x|\mu_e(\hat{x}))$ . Third row: reconstructions from sampled  $z$ , i.e.  $\hat{z} \sim \mathcal{N}(\mu_e(\hat{x}), \sigma_e^2(\hat{x}))$  followed by  $x \sim p^*(x|\hat{z})$ .

The encoder is defined as  $q_\phi(z|x) = \mathcal{N}(x|\mu_e(x), \text{diag}(\sigma_e^2(x)))$ , where  $\mu_e, \sigma_e \in \mathbb{R}^{100}$  are two outputs of a convolutional neural network with an architecture similar to the architecture of the discriminator used for training the GAN (except the output layer), i.e.,  $q_\phi(z|x)$  is a multivariate Gaussian with diagonal covariance matrix whose parameters depend on  $x$ .

Before we start to learn the VAE, we pre-train the encoder fully supervised by maximizing its conditional log-likelihood  $\mathbb{E}_{p^*(x,z)} \log q_\phi(z|x)$  on examples drawn from the ground truth generating model  $p^*(x,z)$ , i.e. (i) draw  $\hat{z} \sim \mathcal{N}(0, I)$ , and (ii) draw  $\hat{x} \sim p^*(x|\hat{z})$ . The results of pre-training are shown in Fig. 3.

After that we jointly learn the encoder and decoder by maximizing ELBO on  $x$ -samples drawn from the ground truth model. We start the learning with the ground truth decoder  $p^*(x|z)$  and the encoder obtained in the previous step. Two variants are considered for this training: In the first one we keep the image noise  $\sigma_d$  fixed. In the second variant  $\sigma_d$  is learned along with other model parameters. To evaluate the results quantitatively, we compute the Frechet



Figure 4. Visual comparison – images drawn from the original/learned models. Each column corresponds to a particular value of  $z \sim \mathcal{N}(0, I)$ . Top row: the ground truth model, middle row: learned decoder with fixed  $\sigma_d$ , bottom row: decoder with learned  $\sigma_d$ .

Table 1. Summary of the ELBO and FID values. The first row corresponds to the pre-trained encoder: the FID-score is obtained by comparing two image sets, both generated by the ground truth model; the ELBO value corresponds to the VAE composed of the pre-trained encoder and the ground truth decoder.

Experiment	ELBO	FID
optimize conditional likelihood	-364513.78	0.13
optimize ELBO, fixed $\sigma_d$	-5898.94	77.10
optimize ELBO, learned $\sigma_d$	9035.69	117.87

Inception Distances (FID) between the ground truth model  $p^*(x|z)$  and the obtained decoders  $p_\theta(x|z)$  using the code of Seitzer (2020). This is done by generating 200k images from the two compared models. The obtained values are summarized in Tab. 1. Fig. 4 shows images generated by the ground truth model and the two learned models.

To conclude, ELBO optimization harms the decoder considerably as clearly seen both from FID-scores and the generated images. Models with higher ELBO values have worse FID-scores and produce less realistic images.

Table 2. Training and test NELBO values for Text-VAE with different configurations of bits, decoder and encoder. Bold highlights the best encoder choice and underlined bold values are the best decoder-encoder combinations for each bit-length.

Bits	TRAINING								
	dhhidden=0			dhhidden=1			dhhidden=2		
	e1	e2	e3	e1	e2	e3	e1	e2	e3
8	<b>419</b>	429	439	<b>321</b>	390	415	<u><b>325</b></u>	370	421
16	<b>382</b>	398	419	<b>201</b>	329	407	<u><b>164</b></u>	269	413
32	<b>337</b>	358	412	<b>165</b>	189	403	<u><b>132</b></u>	159	411
64	<b>296</b>	324	407	<b>171</b>	189	398	<u><b>134</b></u>	149	409

Bits	TEST								
	dhhidden=0			dhhidden=1			dhhidden=2		
	e1	e2	e3	e1	e2	e3	e1	e2	e3
8	<b>423</b>	429	435	<b>413</b>	421	424	<b>418</b>	423	427
16	<b>409</b>	417	421	<b>404</b>	422	420	<b>410</b>	416	422
32	<b>396</b>	413	416	<b>399</b>	413	418	<b>406</b>	416	421
64	<b>392</b>	411	414	<b>398</b>	413	417	<b>406</b>	417	422

### 4.3. Bernoulli VAE for Text Documents

This experiment compares the training of Text-VAE models discussed in Example 3 with and without our proposed correction. We used the processed version of the 20News-groups data set<sup>4</sup>. The dataset contains bag-of-words representations of documents and is split into a training set with 11269 documents and a test set with 7505 documents. We keep only the 10000 most frequent words in the training set, which is a common pre-processing (each of the omitted words occurs not more than in 10 documents).

To train VAE we used the state-of-the-art unbiased gradient estimator ARM (Yin & Zhou, 2019) and Adam optimizer with learning rate 0.001. We did not use the test set for parameter selection. We train for 1000 epochs using 1-sample ARM and then for 500 more epochs using 10 samples for computing each gradient estimate with ARM. We report the lowest negative ELBO (NELBO) values for the training set and test set during all epochs.

We compare three encoders: **e1**: linear encoder on word counts (the proposed correction), **e2**: deep (2 hidden layers) encoder using word frequencies and **e3**: a linear encoder on frequencies. The encoders are compared for different numbers of latent Bernoulli variables (bits) and different decoder depths. The decoder depth denotes the number of fully connected hidden ReLU layers (0-2). In both the encoder and decoder we use 512 units in hidden layers. The prior work mainly used linear decoders following the ablation study of Shen et al. (2018). Our experiments also suggest that using deep decoders in combination with longer bit-length leads to a significant overfitting. When

the decoder is linear, the posterior distribution is tractable and is linear as well, *i.e.* the VAE model is equivalent to an RBM. We experimentally verify that a linear decoder indeed works better in this case. However, perhaps more surprisingly, we also found out that it works better even for non-linear decoders.

Table 2 show the achieved training and test NELBO values (up to a common constant). We observe across all settings that the simple encoder e1 is consistently better than the more complex encoder e2 which in turn is significantly better than the linear encoder on frequencies e3. We conclude that the use of VAEs with deep encoders based on word frequencies (Chaidaroon & Fang, 2017; Shen et al., 2018; Zamani Dadaneh et al., 2020; Nanculef et al., 2020) is sub-optimal for this dataset. We do not expect additional regularization techniques proposed in these works to change this conclusion. We also observe that a linear *decoder* is the best in the test NELBO for 32 and 64 bits because of a significant overfitting with more complex decoders. This implies that in these cases the best encoder-decoder combination is linear, *i.e.* an RBM model.

## 5. Conclusions

We have analyzed the approximation error of VAEs in the general setting, when both the decoder and encoder are exponential families. This includes commonly used VAE variants as, *e.g.*, Gaussian VAEs and Bernoulli VAEs. We have shown that the subset of generative models consistent with the encoder class is quite restricted and moreover can not be enlarged by using more complex encoder networks as long as encoder's sufficient statistics remain unchanged. In combination with the ELBO objective, this causes an approximation error - the ELBO optimizer is pulled away from the data likelihood optimizer towards this subset. This can be desired as a regularizing effect, *e.g.*, in situations with insufficient training data. However, in most practical cases, it leads to degraded decoders that are falling short of the optimal decoder in the considered class.

We believe that fully exploiting the potential of VAEs and using them, *e.g.*, for semi-supervised learning, requires further efforts towards more expressive but still tractable encoder classes.

## Acknowledgements

D.S. was supported by the German Federal Ministry of Education and Research (BMBF, 01/S18026A-F) by funding the competence center for Big Data and AI "ScaDS.AI Dresden/Leipzig". A.S and B.F gratefully acknowledge support by the Czech OP VVV project "Research Center for Informatics" (CZ.02.1.01/0.0/0.0/16019/0000765).

<sup>4</sup><http://qwone.com/~jason/20Newsgroups/>

The authors gratefully acknowledge the Center for Information Services and HPC (ZIH) at TU Dresden for providing computing time.

## References

Burda, Y., Grosse, R. B., and Salakhutdinov, R. Importance weighted autoencoders. In *ICLR*, 2016.

Chaidaroon, S. and Fang, Y. Variational deep semantic hashing for text documents. In *SIGIR Conference on Research and Development in Information Retrieval*, pp. 75–84, 2017.

Cremer, C., Li, X., and Duvenaud, D. Inference suboptimality in variational autoencoders. In *ICML*, volume 80, pp. 1078–1086, 2018.

Dai, B. and Wipf, D. Diagnosing and enhancing VAE models. In *ICLR*, 2019.

Dai, B., Wang, Y., Aston, J., Hua, G., and Wipf, D. Connections with robust PCA and the role of emergent sparsity in variational autoencoder models. *Journal of Machine Learning Research*, 19(41):1–42, 2018.

Grathwohl, W., Choi, D., Wu, Y., Roeder, G., and Duvenaud, D. Backpropagation through the void: Optimizing control variates for black-box gradient estimation. In *ICLR*, 2018.

He, J., Spokoyny, D., Neubig, G., and Berg-Kirkpatrick, T. Lagging inference networks and posterior collapse in variational autoencoders. In *ICLR*, 2019.

Hjelm, D., Salakhutdinov, R. R., Cho, K., Jojic, N., Calhoun, V., and Chung, J. Iterative refinement of the approximate posterior for directed belief networks. In *Advances in Neural Information Processing Systems*, volume 29, pp. 4691–4699, 2016.

Hoffman, M. D., Blei, D. M., Wang, C., and Paisley, J. Stochastic variational inference. *Journal of Machine Learning Research*, 14(4):1303–1347, 2013.

Inkawich, N. DCGAN tutorial, 2017. URL [https://pytorch.org/tutorials/beginner/dcgan\\_faces\\_tutorial.html](https://pytorch.org/tutorials/beginner/dcgan_faces_tutorial.html).

Kim, Y., Wiseman, S., Miller, A., Sontag, D., and Rush, A. Semi-amortized variational autoencoders. In *ICML*, volume 80, pp. 2678–2687, 2018.

Kingma, D. P. and Welling, M. Auto-encoding variational bayes. In *ICLR*, 2014.

Kingma, D. P., Salimans, T., Jozefowicz, R., Chen, X., Sutskever, I., and Welling, M. Improved variational inference with inverse autoregressive flow. In *NIPS*, volume 29, pp. 4743–4751, 2016.

Lucas, J., Tucker, G., Grosse, R. B., and Norouzi, M. Don’t blame the ELBO! a linear VAE perspective on posterior collapse. In *NIPS*, volume 32, pp. 9408–9418, 2019.

Ñanculef, R., Mena, F. A., Macaluso, A., Lodi, S., and Sartori, C. Self-supervised Bernoulli autoencoders for semi-supervised hashing. *CoRR*, abs/2007.08799, 2020.

Rainforth, T., Kosioruk, A. R., Le, T. A., Maddison, C. J., Igl, M., Wood, F., and Teh, Y. W. Tighter variational bounds are not necessarily better. In *ICML*, volume 80, pp. 4274–4282, 2018.

Salakhutdinov, R. and Hinton, G. Semantic hashing. *Int. J. Approx. Reasoning*, 50(7):969–978, July 2009.

Seitzer, M. pytorch-fid: FID Score for PyTorch. <https://github.com/mseitzer/pytorch-fid>, August 2020. Version 0.1.1.

Shen, D., Su, Q., Chapfuwa, P., Wang, W., Wang, G., Henao, R., and Carin, L. NASH: Toward end-to-end neural architecture for generative semantic hashing. In *Annual Meeting of the Association for Computational Linguistics*, pp. 2041–2050, jul 2018.

Sicks, R., Korn, R., and Schwaar, S. A generalised linear model framework for  $\beta$ -variational autoencoders based on exponential dispersion families. *CoRR*, 2021.

Sønderby, C. K., Raiko, T., Maaløe, L., Sønderby, S. K., and Winther, O. Ladder variational autoencoders. In *Advances in Neural Information Processing Systems*, volume 29, pp. 3738–3746, 2016.

Tucker, G., Mnih, A., Maddison, C. J., Lawson, J., and Sohl-Dickstein, J. REBAR: Low-variance, unbiased gradient estimates for discrete latent variable models. In *NIPS*, pp. 2627–2636. 2017.

Yin, M. and Zhou, M. ARM: Augment-REINFORCE-merge gradient for stochastic binary networks. In *ICLR*, 2019.

Zamani Dadaneh, S., Boluki, S., Yin, M., Zhou, M., and Qian, X. Pairwise supervised hashing with Bernoulli variational auto-encoder and self-control gradient estimator. In *UAI*, volume 124, pp. 540–549, 2020.